

## A Comparison of Sulfur- and Oxygen-Modified Mo(111) Surfaces for Methylcyclopropane Hydrogenolysis: Evidence for Participation by Subsurface Atoms in the Active Site

M. S. TOUVELLE<sup>1</sup> AND P. C. STAIR

*Department of Chemistry, Northwestern University, Evanston, Illinois 60208-3113*

Received January 21, 1992; revised July 23, 1992

The catalytic hydrogenolysis of methylcyclopropane has been studied over the Mo(111) crystal plane as a function of preadsorbed atomic sulfur and oxygen coverage. The selectivities for the single hydrogenolysis products, isobutane and *n*-butane, and for the double hydrogenolysis products, methane, propane, and ethane, were the same for sulfur- and oxygen-modified surfaces and independent of modifier coverage. Sulfur and oxygen acted as poisons for the hydrogenolysis activity. The activity decreased linearly with both sulfur and oxygen coverage, but the slope of the activity decay with sulfur was three times that with oxygen. The zero activity intercept corresponded to ca.  $6 \times 10^{14}$  S atoms/cm<sup>2</sup> (one sulfur atom per unit cell) and ca.  $20 \times 10^{14}$  O atoms/cm<sup>2</sup> (three oxygen atoms per unit cell). Examination of structural models for the Mo(111) surface suggests that molybdenum atoms in the second or even third layers must participate in the active site for hydrogenolysis. © 1993 Academic Press, Inc.

### A. INTRODUCTION

Electronegative elements have been observed to inhibit the reaction rates of many catalyzed reactions when added to well-defined transition metal surfaces. Examples of some of these reactions are CO methanation over the S/Ni(100) (1, 2), P/Ni(100) (1), S/Rh(111) (3), S/Ru(0001) (4), S/W(110) (5), and S/Mo(100) (6) surfaces; CO<sub>2</sub> methanation over the S/Ni(100) (7) surface; cyclopropane hydrogenolysis over the S/Ni(100) (8), S/Ni(111) (8), S/Mo(100) (9), O/Mo(100) (9), and C/Mo(100) (9) surfaces; ethane hydrogenolysis over the S/Ru(0001) (4) surface; methylcyclopropane hydrogenolysis over the O/Mo(111) (10) surface; propene metathesis over the O/Mo(100) (11) surface; thiophene hydrodesulfurization over the S/Mo(100) (12); acetylene cyclization to benzene over the S and Cl/Pd(111), Pd(100), and Pd(110) (13) surfaces; and the water–gas shift reaction ( $\text{H}_2\text{O} + \text{CO} \rightarrow \text{H}_2 + \text{CO}_2$ )

over the S/Cu(111) (14) surface. The poisoning mechanism, however, can vary from a simple, site-blocking effect as suggested for the water–gas shift reaction on sulfur-modified Cu(111) (14), to a long-range, electronic interaction as has been proposed for the sulfur- and phosphorus-modified Ni(100) (1, 2) surfaces.

Temperature-programmed desorption experiments have also addressed the steric and electronic effects of electronegative adsorbates on the adsorption of small molecules on transition metal single-crystal surfaces. For example, it has been observed that the presence of Cl, S, and P causes a reduction of the sticking coefficient, the adsorption bond strength, and the adsorption capacity of the Ni(100) surface for CO and H<sub>2</sub> (15–20). In addition, the poisoning effect becomes more prominent with increasing electronegativity of the preadsorbed adatoms. Related studies have been carried out in the presence of C and N atoms. These modifiers have the same electronegativities as S and Cl, 2.5 and 3.0, respectively. In comparing the results for C and N (which both have covalent radii of

<sup>1</sup> Present address: Exxon Research and Development, P.O. Box 2226, Baton Rouge, LA 70821-2226.

$\sim 0.75$  Å) and for S and Cl (which both have covalent radii of  $\sim 1.0$  Å), it was noted that electronegativity effects dominate the poisoning of chemisorption by surface modifiers with similar atomic size and which occupy the same adsorption sites (21). When the modifiers have different atomic size but the same electronegativity (S and C, Cl and N), the poisoning effect becomes less pronounced with decreasing modifier size.

The results of an investigation of the adsorption of Lewis bases,  $\text{NH}_3$ ,  $(\text{CH}_3)_2\text{O}$ , propene, and ethene, and Lewis acids, CO and 3,3,3-trifluoropropene on C- and S-modified Mo(100) surfaces (22), are in agreement with the results for Ni(100). Desorption energies for the various molecules were much higher for the C-modified Mo(100) surfaces than for the S-modified surface. This was explained by the fact that S protrudes much higher above the surface than C (1.0 vs 0.3 Å) and allows less interaction of the probe molecules with the Mo surface atoms.

TPD experiments and reaction studies have shown that both steric and electronic effects can be important in the poisoning mechanisms of electronegative adatoms on transition metal surfaces. The focus of this paper is to address the relative importance of size and electronic effects on the methylcyclopropane (MCP) hydrogenolysis reaction over the sulfur- and oxygen-modified Mo(111) surfaces. Hydrogenolysis of MCP over O/Mo(111) surfaces has been reported previously, and oxygen was proposed to have a simple, site-blocking effect on the reaction rate (10). A comparison of poisoning by sulfur and oxygen surface modifiers is employed to gain a better understanding of the nature of the active site for MCP hydrogenolysis on the Mo(111) surface.

#### B. METHODS

Experiments were performed in a UHV chamber (base pressure of  $2 \times 10^{-10}$  Torr) equipped with two ion pumps and a titanium sublimator. The chamber is also equipped with a quadrupole mass spectrometer, LEED optics, 0–5 kV ion gun, microcapil-

lary array doser, cylindrical mirror analyzer for Auger electron spectroscopy, and a 100-cc-volume high-pressure reactor. Schematic diagrams of the UHV chamber and high-pressure reactor have been presented previously (9).

The Mo single crystal was oriented to within  $\pm 1^\circ$  of the (111) plane. The crystal was polished with successively finer grades of SiC, diamond paste, and alumina (Buehler) down to  $0.03 \mu\text{m}$  and then bulk cleaned of carbon and sulfur by heating in  $5 \times 10^{-7}$  Torr  $\text{O}_2$  at ca. 1500 K for 48 hr. The sample was mounted edge on to a precision manipulator by spot-welding to stainless-steel support rods. The sample could be heated resistively to 1300–1400 K through the supports. The temperature was monitored by a chromel–alumel thermocouple spotwelded to the side of the crystal away from the stainless-steel support rods.

The oxygen and sulfur modified Mo surfaces were prepared by first cleaning the surface with  $\text{Ar}^+$  sputtering followed by annealing to  $\sim 1300$ – $1400$  K to restore surface order. The oxygen-modified surfaces were prepared by exposing the Mo(111) surface to Matheson Research Grade  $\text{O}_2$  through a microcapillary array doser. To obtain oxygen coverages below  $1.7 \times 10^{15}$  atoms/cm<sup>2</sup>, the dose was performed with the crystal at room temperature, followed by a short anneal at 650 K. The clean Mo(111) surface gave a  $p(1 \times 1)$  LEED pattern with quasi-hexagonal symmetry. No ordered O overlayer structures could be observed from room-temperature adsorption. The substrate spots decreased in intensity with a concomitant increase in background intensity during oxygen adsorption. The samples were annealed at 650 K because the Mo(111) surface facets with moderate oxygen coverages and annealing temperatures  $> 1000$  K (23–26). There was no LEED evidence for faceting under the conditions employed here. No LEED patterns were observed for surfaces with oxygen coverages  $> 1.3 \times 10^{15}$  atoms/cm<sup>2</sup> at energies  $< 200$  eV. To obtain O coverages above  $1.7 \times 10^{15}$  atoms/cm<sup>2</sup>, it

was necessary to perform the dosing with the crystal at 650 K.

The sulfur-modified surfaces were prepared by exposing the Mo(111) surface to H<sub>2</sub>S through a microcapillary array doser followed by annealing to 425–525 K to desorb H<sub>2</sub>. Care was taken not to heat the sample above 875 K, as facetting occurs when sulfur is adsorbed. The highest sulfur coverage achieved was  $0.96 \times 10^{15}$  atoms/cm<sup>2</sup>. This is similar to that found for Mo(100), where the saturation sulfur coverage is  $1.0 \times 10^{15}$  atoms/cm<sup>2</sup> (27–29). As was the case with O-modified surfaces, no ordered S overlayer structures were observed.

Oxygen coverages were determined by Auger using the O(503 eV)/Mo(221 eV) peak–height ratio which was calibrated against an Mo(100) surface having 0.5 monolayers of atomic oxygen and 0.5 monolayers of atomic carbon prepared by saturating the clean surface with dissociated CO ( $\beta$ -CO) (30). Sulfur coverages were determined by Auger using the S(152 eV)/Mo(221 eV) peak–height ratio, which was calibrated against an Mo(100) surface with atomic carbon and sulfur prepared by dissociative adsorption of CS<sub>2</sub>. The sulfur to carbon atomic surface ratio was assumed to be 2 : 1 (22). The coverages assigned to the various LEED patterns observed for sulfur and oxygen on Mo(100) using the calibrated Auger data are in excellent agreement with previous results reported in the literature (28, 29, 31). Two corrections had to be made to the sensitivity factor to obtain accurate modifier coverages for the (111) surface. The first correction took into account the different unit cell areas for the (111) and (100) surfaces which are 17.07 and 9.86 Å<sup>2</sup>, respectively. The second correction involved a small difference in the calculated Mo(221 eV) Auger peak intensity for the two surfaces. Oxygen and sulfur coverages reported here were the average of three measurements taken at three different spots on the crystal prior to reaction. Three measurements were also taken after the reaction to

check for carbon deposition and/or oxide reduction. The coverage determination by Auger should be accurate to  $\pm 1 \times 10^{14}$  atoms/cm<sup>2</sup>.

Reaction conditions used were 5 Torr of MCP, 750 Torr of H<sub>2</sub>, and a crystal temperature of 373 K. Specifics concerning reactant purification, reactor and sample passivation, and reaction procedures have been described previously (9, 10).

### C. RESULTS

Methylcyclopropane hydrogenolysis was observed at a temperature of 373 K on the initially clean Mo(111) surface and surfaces modified with sulfur coverages between 0 and  $0.96 \times 10^{15}$  atoms/cm<sup>2</sup>; 0.1–15% MCP conversion occurred over a 2-hr period at 373 K. Products detected were isobutane, *n*-butane, propane, ethane, and methane. 1-Butene and propene also were detected throughout the run on the surface with  $0.96 \times 10^{15}$  S atoms/cm<sup>2</sup>, indicating decreased hydrogenation activity. The decrease in hydrogenation activity was seen previously on heavily oxidized Mo(111) surfaces (10). Sulfur coverages before and after a reaction were identical within  $\pm 1 \times 10^{14}$  S atoms/cm<sup>2</sup>. Carbon deposition was detected by Auger following the reaction. In general, the amount of carbon deposited decreased with increasing sulfur precoverage as illustrated in Fig. 1.

Rates of reaction were computed from plots of product accumulation as a function of time. Since no deactivation was observed for isobutane, methane, propane, or ethane product accumulation curves, rates were computed from a linear least-squares fit to the data. In some cases, for *n*-butane, there was an apparent large initial rate followed by a decrease in rate which then remained constant for the remainder of the run (Fig. 2). This feature was considered to be an artifact and was probably due to inaccuracies in subtracting the large *n*-butane and 1-butene impurities present in the reactant mixture. The amount of *n*-butane produced from hydrogenolysis was generally  $\leq$  the

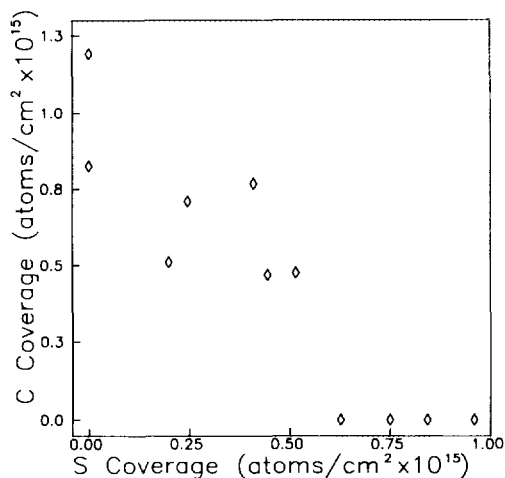


FIG. 1. Carbon coverage following reaction as function of sulfur precoverage.

amount of *n*-butane plus 1-butene initially present as impurities. In calculating *n*-butane TOFs, this initial jump was ignored and a linear least-squares fit was used for the remainder of the data. All top-layer Mo atoms ( $n_s = 5.85 \times 10^{14}$  Mo atoms/cm<sup>2</sup>) were counted in the computation of TOFs for the initially clean Mo(111) surface as well as the sulfur-modified surfaces. This proce-

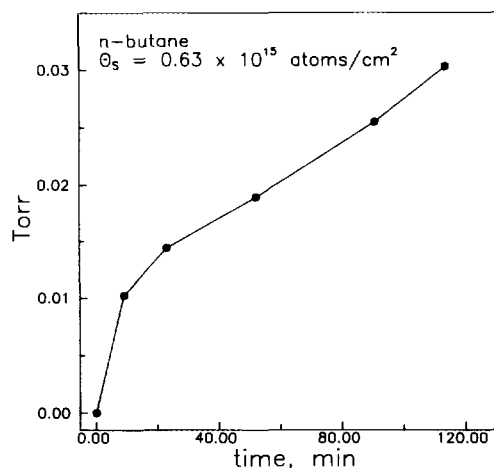


FIG. 2. *n*-Butane product accumulation curve for  $\theta_s = 0.63 \times 10^{15}$  atoms/cm<sup>2</sup> illustrating the large initial increase in rate followed by a leveling off.

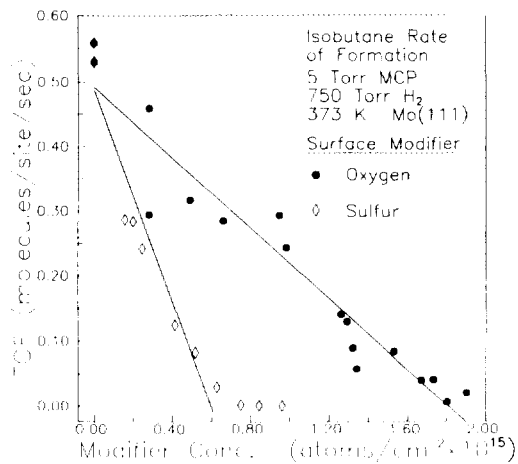


FIG. 3. Comparison of the decrease in the rate of isobutane formation with increasing sulfur and oxygen coverage.

cedure only gives accurate TOFs for all surfaces if the active site density is constant for all surfaces investigated.

Turnover frequencies for hydrogenolysis of methylcyclopropane to form isobutane, methane, propane, and ethane as a function of sulfur and oxygen modifier coverage are compared in Figs. 3-6. The activities decrease linearly with coverage for both mod-

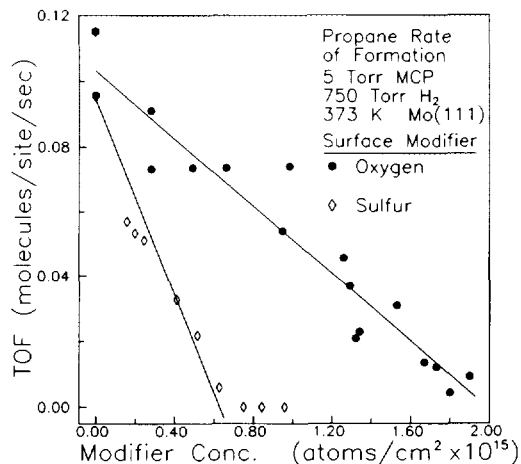


FIG. 4. Comparison of the decrease in the rate of propane formation with increasing sulfur and oxygen coverage.

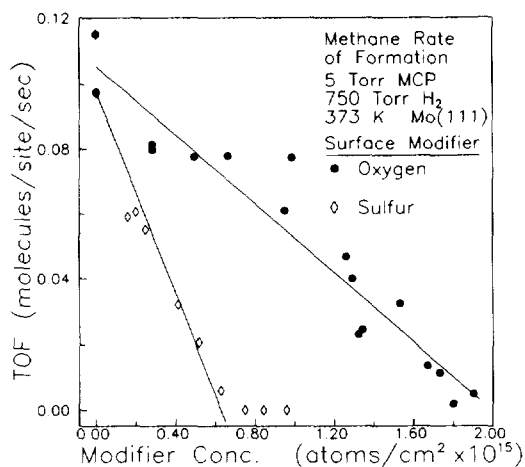


FIG. 5. Comparison of the decrease in the rate of methane formation with increasing sulfur and oxygen coverage.

ifiers. On the sulfur-modified surface, the zero rate intercept was at a sulfur coverage of  $\sim 0.6 \times 10^{15}$  S atoms/cm<sup>2</sup> (i.e., one S atom per unit cell), whereas on the oxygen-modified surface, the corresponding coverage was  $\sim 2 \times 10^{15}$  O atoms/cm<sup>2</sup> (i.e., approximately three O atoms per unit cell). The activity for *n*-butane formation also decays linearly with sulfur coverage with the

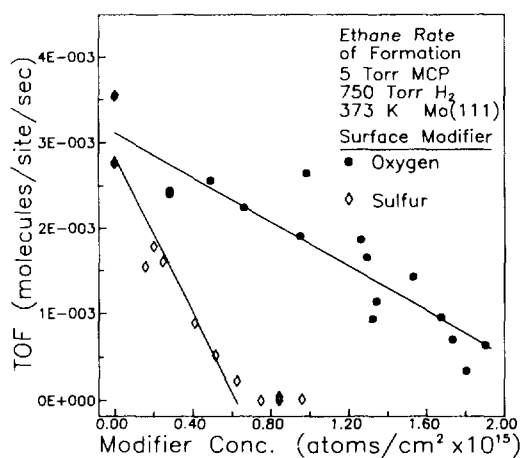


FIG. 6. Comparison of the decrease in the rate of ethane formation with increasing sulfur and oxygen coverage.

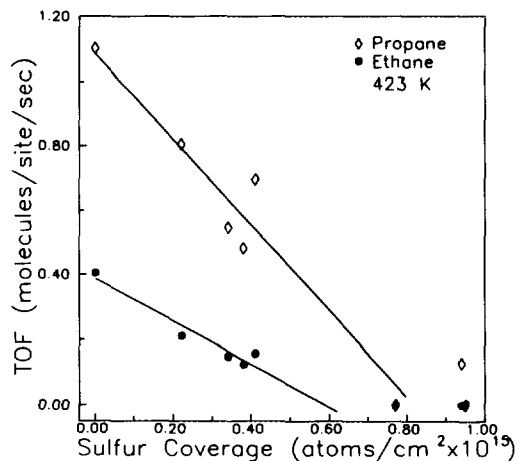


FIG. 7. Turnover frequencies for cyclopropane hydrogenolysis products, propane and ethane, as a function of sulfur coverage. The straight lines are least-squares fits to the data for sulfur coverages below  $0.5 \times 10^{15}$  atoms/cm<sup>2</sup>. Reaction conditions were 40 Torr CP, 715 Torr H<sub>2</sub>, and a crystal temperature of 423 K.

same zero-rate intercept. However, a comparison of activities for *n*-butane formation between sulfur and oxygen modifiers is not meaningful, since in the latter case there is a change in the catalytic mechanism and actually an increase in activity corresponding to the formation of oxide at an oxygen coverage in the range  $1.0\text{--}1.5 \times 10^{15}$  cm<sup>2</sup> (10). Although there is limited data, similar behavior was observed for cyclopropane hydrogenolysis over sulfur-modified Mo(111) at a temperature of 423 K (Fig. 7). The zero rate intercepts for ethane formation and propane formation were at  $\sim 0.6 \times 10^{15}$  S atoms/cm<sup>2</sup> and  $\sim 0.8 \times 10^{15}$  S atoms/cm<sup>2</sup>, respectively.

Methane and propane TOFs were identical within experimental error on the sulfur-modified surfaces as they were on the oxygen-modified surfaces (10) and as reported in the literature for supported Mo catalysts (32, 33). The oxygen modifiers suppress the rate of formation of isobutane and the three double hydrogenolysis products linearly with increasing modifier coverage. In addi-

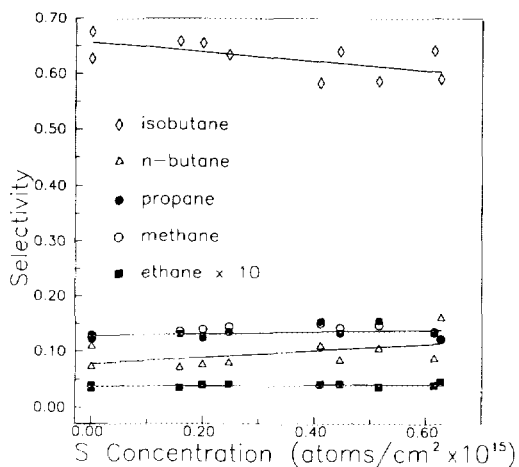


FIG. 8. Selectivities for all hydrogenolysis products as a function of sulfur precoverage.

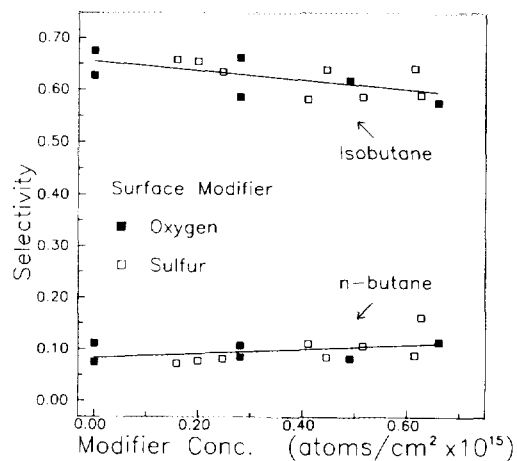


FIG. 9. Comparison of the effect of sulfur and oxygen surface modifiers on the selectivity for isobutane and *n*-butane formation.

tion the zero rate intercept was the same for these products. These facts suggest that the active site for isobutane production is the same as the active site for the formation of double hydrogenolysis products.

Selectivities for all hydrogenolysis products as a function of sulfur coverage are shown in Fig. 8. Selectivities are not shown for sulfur coverages greater than  $0.63 \times 10^{15}$  atoms/cm<sup>2</sup> because the rates were extremely low and led to large errors in computing selectivities. Selectivities ( $S_x$ ) were calculated by defining

$$S_{C_2H_6} + S_{CH_4} + S_{C_3H_8} + S_{i-C_4H_{10}} + S_{n-C_4H_{10}} = 1,$$

where

$$S_x = \frac{TOF_x}{\text{Total TOF}}$$

The distribution remained essentially constant at ca. 63% isobutane, 10% *n*-butane, 13% propane, 13% methane, and 0.4% ethane. Although the rates on the sulfur- and oxygen-modified surfaces were different, the selectivities were the same. Selectivities for the hydrogenolysis products on both the sulfur- and oxygen-modified Mo(111) surfaces up to a coverage of  $0.65 \times 10^{15}$  atoms/

cm<sup>2</sup> are compared in Figs. 9 and 10. The data for methane was almost identical to that of propane and is omitted for clarity.

#### D. DISCUSSION

The results presented here agree with previous results for the hydrogenolysis of cyclopropane on an initially clean Mo(100) surface and surfaces chemically modified with

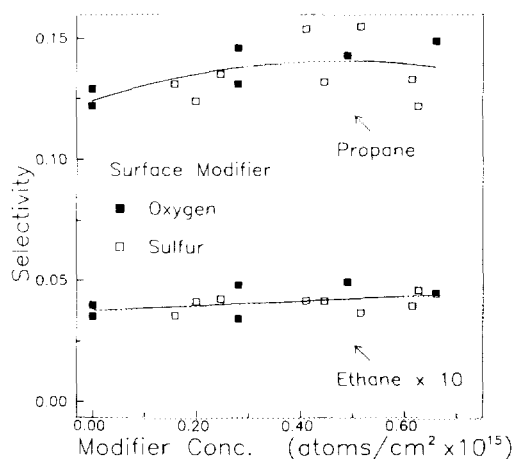


FIG. 10. Comparison of the effect of sulfur and oxygen surface modifiers on the selectivity for propane and ethane formation.

one monolayer (ML) of oxygen and one ML of carbon (9). The active sites for this reaction were assigned to be fourfold hollows of metallic character present in high concentration on the initially clean surface and as defects on the chemically modified surfaces. Interestingly, the activation energy and product distribution were the same on all three surfaces. The activity of the clean surface, however, was higher than that of the C- and O-modified surfaces. The results for MCP hydrogenolysis over sulfur-modified Mo(111) surfaces are also consistent with those obtained for oxygen-modified Mo(111) surfaces (10). A constant product distribution below  $1 \times 10^{15}$  O atoms/cm<sup>2</sup> and  $0.65 \times 10^{15}$  S atoms/cm<sup>2</sup>, and a decrease in activity with oxygen and sulfur precoverage, also suggest an active site of metallic character.

The main difference between the sulfur and oxygen modified Mo(111) surfaces is that the reaction rates decreased to zero at a sulfur coverage which was approximately one-third the corresponding oxygen coverage. The mechanism of catalyst poisoning by an atomic species has generally been assigned either to a physical blocking of the active site or an electronic modification which renders the site incapable of catalyzing the reaction. In this context, the change in poisoning efficiency between sulfur and oxygen may be attributed either to differences in their electronegativity or their size. Sulfur has a covalent radius of 1.02 Å and an electronegativity of 2.5, while oxygen has a covalent radius of 0.7 Å and an electronegativity of 3.5. The relative importance of size and electronic perturbation in poisoning will be discussed below.

While it is certain there is some surface electronic perturbation upon adsorption of sulfur due to charge transfer effects with nearest neighbors and changes in the Fermi level local density of states (LDOS), it is unlikely that this is the major factor determining the differences between the sulfur and oxygen modified surfaces. The fact that oxygen is more electronegative than sulfur

implies that there would be more charge transfer from the Mo to oxygen than from Mo to sulfur. The rates would be expected to be more sensitive to oxygen coverage and, in fact, the opposite occurs. A reaction which provides a good example of the effect of the electronegativity of an adatom on its poisoning efficiency is CO methanation on Ni(100) (34). Sulfur was found to effectively poison 10 Ni atoms, whereas phosphorus, which is the same size as sulfur, only poisoned the four nearest neighbor metal atoms. Phosphorus is less electronegative than S (2.1 vs 2.5) and this difference was suggested to be responsible for the difference in CO methanation rates on the two modified surfaces.

Consistent with the CO methanation poisoning experiments, Feibelman and Hamann (35, 36) have shown in calculations that electronegative adatoms (S, P, Cl) cause a reduction of the LDOS near the Fermi level which might be extended over distances greater than the next nearest neighbor. The strength of the effect was found to increase with increasing additive electronegativity. This argument would also predict a faster decrease in the hydrogenolysis rate over the oxygen-modified surfaces as compared to the sulfur-modified surfaces, which is the opposite of the experimental results.

Maclaren *et al.* (37, 38) have pointed out that electronegativity differences will explain the trends in poisoning only when the vertical spacings between the metal and adatoms are similar for both adatoms. The height of a catalytic poison above the surface was found to have a much larger effect than electronegativity on the LDOS. For example, sulfur was found to cause a large reduction in the LDOS of Ni, whereas carbon (having the same electronegativity as sulfur) caused only a small reduction. The magnitude of reduction was attributed to the differences in vertical spacings between Ni and S vs Ni and C. Carbon resides 0.1 Å above the top Ni layer, whereas S resides 1.3 Å above the top layer. It was also found

that if the Ni–C distance was changed to 1.3 Å, the poisoning effect of C was increased to the same level as that of S. The authors also concluded that the effect was not due to simple electrostatic screening, because they considered neutral species, but rather to the ability of the poison-induced electronic perturbations to propagate across the surface.

Finally, Lang *et al.* (39) have tried to explain the effect of additives by the sign and magnitude of the electrostatic potential around an adatom outside a jellium surface. P, S, Cl, and O showed the same trend in poison strength as predicted by Feibelman and Hamann. The increase of the poison strength in the sequence P, S, Cl, however, was attributed to an increase in the electrostatic potential associated with the adatom. The range of this type of interaction was found to be short (~3–4 Å), on the order of the screening length of the metal. Interestingly, O (electronegativity of 3.5) was found to have a weaker effect than Cl (electronegativity of 3.0) which was attributed to the smaller size of O (0.99 Å vs 0.73 Å). It was suggested that the electrostatic potential was more efficiently screened for O because it was imbedded in the jellium. It has been noted that since this model considers only direct electrostatic interactions, it would be more applicable for explaining the effect of highly polarized adatoms such as alkalis (39, 40).

The work of Maclaren and coworkers and Lang *et al.* both conclude that the size of the adatom is more important in determining the strength of the poisoning effect than the electronegativity. In an earlier paper, cyclopropane hydrogenolysis over C- and S-modified Mo(100) surfaces was investigated (9). It is known that C resides ~0.3 Å above the top Mo layer, whereas S resides 1 Å above the top layer. The calculations of Maclaren *et al.* are in agreement with the CP hydrogenolysis data in that the 1 ML C-modified Mo(100) surface was active for hydrogenolysis and the 0.8 ML S-modified surface was inactive. The results of Lang's comparison

of O and Cl modifiers are very similar to what was observed for the O- and S-modified Mo(111) surfaces. The addition of oxygen was found to have less of a poisoning effect on MCP hydrogenolysis than S, even though oxygen is more electronegative than sulfur. The surface structures for the O/Mo(111) and S/Mo(111) systems are not known; however, because oxygen is smaller than sulfur, the O–Mo distance will almost certainly be less than the S–Mo distance. From Maclaren's and Lang's calculations one would predict lower activity for the S-modified Mo(111) surfaces in agreement with what is observed. Similarly, studies of CO adsorption on S/Ni(111) and O/Ni(111) have shown that the range of the effect and the strength of the perturbations depend more strongly on the actual distance of the modifier from the surface than on its electronegativity (40). Thus, it appears that steric and short-range electronic effects rather than long-range electronic perturbations are the dominant poisoning mechanisms for the systems studied here.

A simple, commonly used expression to determine the number of sites inactivated by a poison is

$$r = r_0(1 - a\theta),$$

where  $r_0$  is the rate when no poison is present on the surface,  $\theta$  is the coverage of the poison, and  $a$  is the number of sites inactivated per poison atom (41). If the MCP hydrogenolysis data are normalized such that  $r_0 = 1$ , the slope of reaction rate decay can be fit to  $(1 - \theta_s)$  for the sulfur-modified Mo(111) surfaces and  $(1 - 0.33\theta_o)$  for the oxygen-modified surfaces. Rates and coverages were calculated using only the top layer Mo atoms. Thus, one monolayer is equivalent to  $5.85 \times 10^{14}$  atoms/cm<sup>2</sup> for the Mo(111) surface. In addition, only rate data from sulfur-modified surfaces with coverages less than  $7 \times 10^{14}$  S atoms/cm<sup>2</sup> were fit; rates on surfaces with larger sulfur coverages were essentially zero. Lines corresponding to these fits are shown in Figs. 3–6. According to these models, one Mo atom is poisoned per S atom and



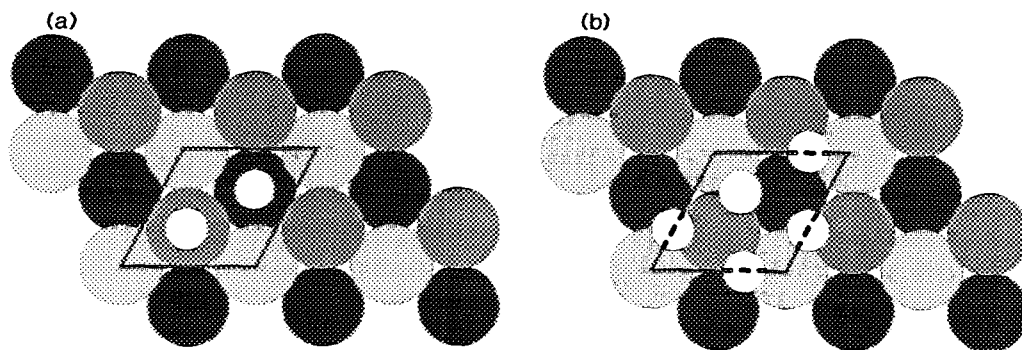


Fig. 11. (a) The Mo(111) surface showing adsorption on top of second and third layer atoms. (b) The Mo(111) surface showing adsorption at threefold sites. The unit cell is drawn for clarity. Small, open circles—O; light gray circles—1st layer Mo; dark gray circles—2nd layer Mo; black circles—3rd layer.

0.33 Mo atoms are poisoned per O atom. It is hard to rationalize how three oxygen atoms would be required to poison each top-layer molybdenum while only one sulfur atom does the job. It is more likely that counting only top-layer atoms is incorrect. When second- and third-layer atoms are also used in calculating rates and coverages, the decays are fit by  $(1 - 3\theta)$  and  $(1 - \theta)$  for the sulfur- and oxygen-modified surfaces, respectively. In this case the surface Mo density is equivalent to  $1.75 \times 10^{15}$  atoms/cm<sup>2</sup>. Thus, three Mo atoms per sulfur atom and one Mo atom per oxygen atom are poisoned. This also implies that there are three oxygen atoms per unit cell at a coverage of  $1.75 \times 10^{15}$  atoms/cm<sup>2</sup> (ca. the zero rate intercept). If oxygen was adsorbed in the threefold hollow sites (i.e., on top of second- and third-layer Mo atoms), only two oxygens per unit cell would be allowed (Fig. 11a). Threefold adsorption sites (formed by first-, second-, and third-layer Mo atoms) have been proposed for the O/Mo(111) system (42) and bridge sites for the O/W(111) system (43). If these sites are preferred, at least three oxygen atoms per unit cell would be allowed. Figure 11b illustrates a possible configuration for oxygen adsorbed at threefold sites which allows three oxygen atoms per unit cell. Similar results are obtained if oxygen is adsorbed at bridge sites between second- and third-layer atoms.

In addition, the sites in the interior of the threefold hollows provide a configuration for threefold and twofold oxygen coordination to molybdenum atoms. Atop site bonding provides only for a coordination number of one. Finally, oxygen atoms are small enough that they will not protrude above the top-layer Mo atoms when they are adsorbed at any of the higher coordination sites. It should be noted that oxygen can and does penetrate transition metal surfaces (42, 44). Thus, it may not be necessary to account for all of the oxygen as surface oxygen; some of it may be subsurface.

As mentioned earlier, the zero rate intercept for the sulfur-modified surface corresponded to a coverage of one sulfur atom per unit cell. If one assumes that sulfur adsorbs at threefold sites or bridge sites (as we did for oxygen) then at a coverage of one sulfur atom per unit cell the top Mo layer atoms are likely to be accessible to reactant. Thus, the top-layer, low-coordination-number Mo atoms are probably not the active metal atoms for the MCP reaction. This implies that the high-coordination-number second- and third-layer Mo atoms in the interior of the threefold hollows are associated with the active site.

High-coordination-number atoms have been proposed for ammonia synthesis as the active metal atoms in the dissociation of N<sub>2</sub>

over Fe surfaces (45). The dissociation probability of  $N_2$  was higher on the open Fe(111) surface (with sevenfold coordination sites exposed) than on the close-packed Fe(110) surface (46). The rate of the Fe(111) surface for ammonia synthesis was found to be 500 times greater than that of the Fe(110) surface. Similar results have been reported for rhenium surfaces (47). High-coordination-number atoms have also been proposed as the most active ones for  $H_2$ - $D_2$  exchange (48) and alkane hydrogenolysis (49, 50) over various stepped and kinked Pt surfaces.

Falicov and Somorjai (51) suggested that high-coordination transition metal atoms are catalytically active because they are susceptible to low-energy electronic fluctuations such as electron configuration fluctuations. A good catalyst forms weakly bound intermediates which can readily react and desorb. Falicov's theory suggests that atoms which can readily undergo electronic fluctuations can easily form catalytically active intermediates and once formed will allow reaction and desorption to occur. If electronic fluctuation is inhibited, either a stabilized intermediate will be formed or no reaction will occur at all. It was shown that transition metal atoms which are bulk-like (have a high coordination number) can more readily undergo these fluctuations than low coordination atoms.

One final point to be noted is that this type of a poisoning study confirms the fact that the reaction is taking place on the well-defined front face of the crystal. The fact that both MCP and CP hydrogenolysis rates are completely poisoned at a coverage of one sulfur atom per unit cell is evidence that the catalytic activity is not being dominated by edge sites or sites on the back side of the Mo crystal.

#### E. CONCLUSIONS

Selectivities for the single hydrogenolysis products of MCP, isobutane and *n*-butane, and the double hydrogenolysis products, methane, propane, and ethane, were identical whether an initially clean Mo(111) sur-

face, an S-modified Mo(111) surface, or an O-modified Mo(111) surface was used as a catalyst. These products were formed on metallic Mo, and preadsorbed sulfur and oxygen acted as poisons for the hydrogenolysis reactions. The fact that the rate decay is linear for both oxygen- and sulfur-modified surfaces and that the number of Mo atoms blocked per adatom is small (one for oxygen and three for sulfur) is strong evidence that the poisoning mechanism can be understood in terms of a simple, site-blocking model and that the ensemble required for reaction is small. It was also suggested that second- and third-layer, high-coordination-number Mo atoms were associated with the active site.

#### ACKNOWLEDGMENT

This material is based upon work supported by the National Science Foundation under Award CHE-882781.

#### REFERENCES

1. Goodman, D. W., *Appl. Surf. Sci.* **19**, 1 (1984).
2. Goodman, D. W., and Kiskinova, M., *Surf. Sci.* **105**, L265 (1981).
3. Goodman, D. W., in "Heterogeneous Catalysis Proceedings of IUCCP Conference" (B. L. Shapiro, Ed.), p. 230. Dept. of Chem., Texas A&M Univ., 1984.
4. Peden, C. H. F., and Goodman, D. W., *Ind. Eng. Chem. Fundam.* **25**, 58 (1986).
5. Szuromi, P. D., Kelley, R. D., and Madey, T. E., *J. Phys. Chem.* **90**, 6498 (1986).
6. Logan, M., Gellman, A., and Somorjai, G. A., *J. Catal.* **94**, 60 (1985).
7. Peebles, D. E., Goodman, D. W., and White, J. M., *J. Phys. Chem.* **87**, 4378 (1983).
8. Goodman, D. W., *J. Vac. Sci. Technol. A* **2**, 873 (1984).
9. Kellogg, D. S., Touvelle, M. S., and Stair, P. C., *J. Catal.* **120**, 192 (1989).
10. Touvelle, M. S., and Stair, P. C., *J. Catal.* **130**, 556 (1991).
11. Wang, L. P. and Tysoe, W. T., *Catal. Lett.* **6**, 111 (1990).
12. Gellman, A. J., Bussell, M. E., and Somorjai, G. A., *J. Catal.* **107**, 103 (1987).
13. Logan, M. A., Rucker, T. G., Gentle, T. M., Muettterties, E. L., and Somorjai, G. A., *J. Phys. Chem.* **90**, 2709 (1986).
14. Campbell, C. T., and Koel, B. E., *Surf. Sci.* **183**, 100 (1987).

15. Kiskinova, M., and Goodman, D. W., *Surf. Sci.* **108**, 64 (1981).
16. Goodman, D. W., and Kiskinova, M., *Surf. Sci.* **105**, L625 (1981).
17. Hardegee, E. L., Ho, P., and White, J. M., *Surf. Sci.* **165**, 488 (1986).
18. Johnson, S., and Madix, R. J., *Surf. Sci.* **108**, 77 (1981).
19. Madix, R. J., Lee, S. B., and Thornburg, M., *J. Vac. Sci. Technol. A* **1**, 1254 (1983).
20. Madix, R. J., Thornburg, M., and Lee, S. B., *Surf. Sci.* **133**, L447 (1983).
21. Kiskinova, M., and Goodman, D. W., *Surf. Sci.* **109**, L555 (1981).
22. Deffeyes, J. E., Smith, A. H., and Stair, P. C., *Appl. Surf. Sci.* **26**, 517 (1986).
23. Kennett, H. M., and Lee, A. E., *Surf. Sci.* **48**, 606 (1975).
24. Zhang, C., Van Hove, M. A., and Somorjai, G. A., *Surf. Sci.* **149**, 326 (1985).
25. Zhang, C., Gellman, A. J., Farias, M. H., and Somorjai, G. A., *Mater. Res. Bull.* **20**, 1129 (1985).
26. Ferrante, J., and Barton, G. C., NASA TND-4735.
27. Clarke, L. J., *Surf. Sci.* **102**, 331 (1981).
28. Salmeron, M., Somorjai, G. A., and Chianelli, R. R., *Surf. Sci.* **127**, 526 (1983).
29. Maurice, V., Peralta, L., Berthier, Y., and Oudar, J., *Surf. Sci.* **148**, 623 (1984).
30. Felter, T. E., and Estrup, P. J., *Surf. Sci.* **54**, 197 (1976).
31. Bauer, E., and Poppa, H., *Surf. Sci.* **88**, 31 (1979).
32. Burwell, R. L., Jr., and Chung, J., *React. Kinet. Catal. Lett.* **35**, 381 (1987).
33. Chung, J., and Burwell, R. L., Jr., *J. Catal.* **116**, 519 (1989).
34. Goodman, D. W., *Annu. Rev. Phys. Chem.* **37**, 425 (1986).
35. Feibelman, P. J., and Hamann, D. R., *Phys. Rev. Lett.* **52**, 61 (1984).
36. Feibelman, P. J., and Hamann, D. R., *Surf. Sci.* **149**, 48 (1985).
37. Maclaren, J. M., Pendry, J. B., and Joyner, R. W., *Surf. Sci.* **165**, L80 (1986).
38. Maclaren, J. M., Pendry, J. B., and Joyner, R. W., and Meehan, P., *Surf. Sci.* **175**, 263 (1986).
39. Lang, N. D., Holloway, S., and Nørskov, J. K., *Surf. Sci.* **150**, 24 (1985).
40. Kiskinova, M. P., *Surf. Sci. Rep.* **8**, 359 (1988).
41. Andersen, N. T., Topsøe, F., Alstrup, I., and Rostrop-Nielsen, J. R., *J. Catal.* **104**, 454 (1987).
42. Stefanova, P. K., and Marinova, Ts. S., *Surf. Sci.* **200**, 26 (1988).
43. Niehus, H., *Surf. Sci.* **80**, 245 (1979).
44. Lawless, K. R., *Rep. Prog. Phys.* **37**, 231 (1974).
45. Ertl, G., *Catal. Rev. Sci. Eng.* **21**, 201 (1980).
46. Spencer, N. D., Schoonmaker, R. C., and Somorjai, G. A., *J. Catal.* **74**, 129 (1982).
47. Asscher, M., and Somorjai, G. A., *Surf. Sci.* **143**, 1389 (1984).
48. Salmeron, M., Gale, R., and Somorjai, G. A., *J. Chem. Phys.* **67**, 5324 (1977).
49. Gillespie, W. D., Herz, R. K., Petersen, E. E., and Somorjai, G. A., *J. Catal.* **70**, 147 (1981).
50. Davis, S. M., Zaera, F., and Somorjai, G. A., *J. Am. Chem. Soc.* **104**, 7453 (1982).
51. Falicov, L. M., and Somorjai, G. A., *Proc. Natl. Acad. Sci. U.S.A.*, **82**, 2207 (1985).